U-Pb zircon geochronology of granitic and syenitoid rocks across the southern part of the Sveconorwegian orogen

Jenny Andersson (Editor)

June 2012

SGU-rapport 2012:14

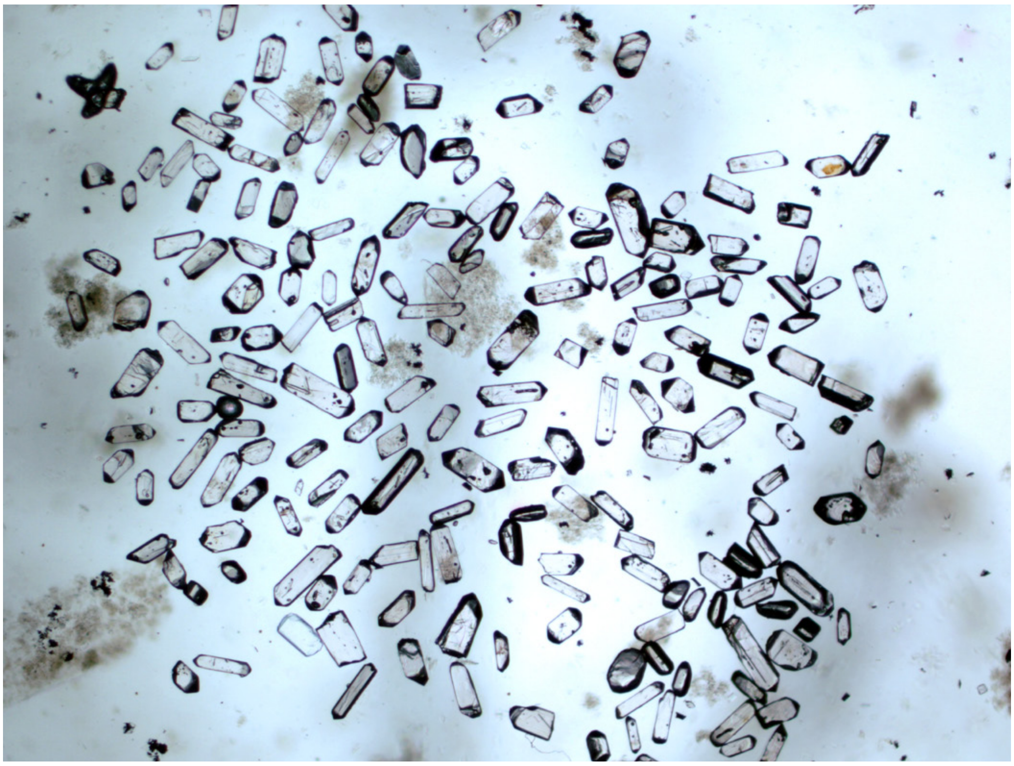

SGU
Sveriges geologiska undersökning
Geological Survey of Sweden

Cover: Photo in optical microscope of polished mount with zircon from a meta-granite at Vättnet, Nordkoster. Image taken prior to U-Pb LA-SF-ICP-MS analysis.

Sveriges geologiska undersökning
Box 670, 751 28 Uppsala
tel: 018-17 90 00
fax: 018-17 92 10
e-post: sgu@sgu.se
www.sgu.se

EDITOR'S PREFACE

Geochronology is a fundamental cornerstone in bedrock mapping. In the Precambrian, the absence of a useful fossil record requires application of radiometric dating methods. The radiometric ages are a prerequisite for understanding how the bedrock is constructed and how rocks are related in space and time. Radiometric age determinations are therefore an integral part of the bedrock mapping programme of the Geological Survey of Sweden. The geochronological data are published as short notes in the report series "SGU-rapporter".

This publication presents U-Pb zircon data from across the eastern part of the Sveconorwegian orogen (as outlined by e.g. Berthelsen 1980 and Bingen et al. 2008, see Fig. 1). The large scale tectonic reconfiguration of crustal scale bedrock units, and the in part deep subduction of crust, has had a fundamental bearing on the character of the bedrock in this part of the shield area. It thus directly governs the usability of rocks for societal applications. The first report by Eliasson et al. (a) presents data from the upper tectonic levels of the Sveconorwegian orogen that forms a boundary between deeply subducted high-grade metamorphic rocks in the west and well preserved igneous rocks in the pre-Sveconorwegian foreland in the east (Fig. 1). The results show that the rocks in the Tokeryd area, north-north-west of Jönköping, are related to strongly metamorphosed and deformed gneissic rocks in the lower tectonic levels of the Sveconorwegian orogen in the west. The second paper by Lundqvist et al. presents time constrains on igneous crystallisation of protoliths to strongly reworked, veined gneisses in the Eastern Segment in the Alingsås area. The results show that the protoliths to the high-grade metamorphic rocks in the western, deeply subducted, lower tectonic levels of the Eastern Segment are linked to well preserved rocks in the upper tectonic levels in the east. It confirms a link with the well preserved intrusion at Tokeryd, described by Eliasson et al. (a) in paper 1, and thus corroborates the parautochthonous nature of the Eastern Segment. The data also help to constrain the outline of the lithotectonic boundary to the overlying allochthonous Idefjorden Terrane for which the link to the pre-Sveconorwegian rocks in the foreland region is unclear. In paper III, Eliasson et al. (b) present data on a structurally young granite intrusion at Nordkoster in the south-western parts of the Idefjorden Terrane. The new data demonstrate a clear

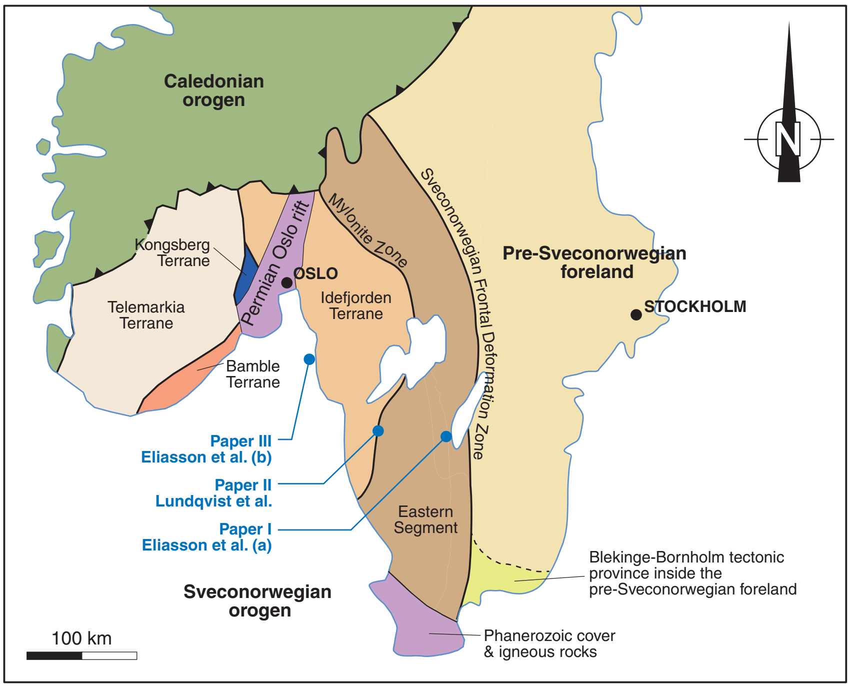

Figure 1. Schematic outline of the Sveconorwegian orogen in the southern Fennoscandian Shield. Outline of orogenic segments in Norway follows Bingen et al. (2008). The location of studied areas are also shown.

link to Gothian orogenesis and overrule a younger Mesoproterozoic affinity. The data also set an upper age constraint for the voluminous mafic dyke swarm of unknown age (Koster dyke swarm of Hageskov 1985) that intrudes the dated granite.

The data in papers one and three were obtained in collaboration between SGU and GEUS (Geological Survey of Denmark and Greenland). This work was made possible by the kind and skillful co-operation of Dirk Frei (former senior advisor at the ICPMS laboratory, Ministry of Climate and Energy, GEUS, Copenhagen) which is gratefully acknowledged. Data in paper two were obtained from beneficial co-operation with the Laboratory for Isotope Geology of the Swedish Museum of Natural History in Stockholm, and the head of NORDSIM, Dr. Martin Whitehouse, and his staff are greatly acknowledged for first class analytical support.

Uppsala, 26th of June 2012
Jenny Andersson

References

Berthelsen, A., 1980: Towards a palinspastic analysis of the Baltic shield. *In* J. Cogne & M. Slansky (Eds.): Geology of Europe from Precambrian to Post-Hercynian Sedimentary Basins. *Int. Geol. Congr., Colloq. C6, Paris*, 5–21.

Bingen, B., Nordgulen, Ø. & Viola, G., 2008: A four-phase model for the Sveconorwegian orogeny, SW Scandinavia. *Norwegian Journal of Geology 88*, 43–72.

Hageskov, B., 1985: Constrictional deformation of the Koster dyke swarm in a ductile sinistral shear zone, Koster islands, SW Sweden. *Bulletin of the Geological Society of Denmark 34*, 151–197.

CONTENTS

U-Pb ZIRCON AGE OF A TIB-2 QUARTZ MONZONITE FROM TOKERYD IN THE PROTOGINE ZONE NORTH-WEST OF JÖNKÖPING, SOUTH CENTRAL SWEDEN

Thomas Eliasson[1], Anders Scherstén[2], Jenny Andersson[3], Ulf Bergström[1] & Andreas Petersson[2]

[1]Geological Survey of Sweden, Guldhedsgatan 5A, SE-413 20 Göteborg, Sweden
[2]Department of geology, Lund university, Sölvegatan 12, SE-223 62 Lund, Sweden
[3]Geological Survey of Sweden, Box 670, SE-751 28 Uppsala, Sweden

Eliasson, T., Scherstén, A., Andersson, J., Bergström, U. & Petersson, A., 2012: U-Pb zircon age of a TIB-2 quartz monzonite from Tokeryd in the Protogine Zone north-west of Jönköping, south central Sweden. *In* J. Andersson (Ed.): U-Pb zircon geochronology of granitic and syenitoid rocks across the southern part of the Sveconorwegian orogen. *SGU-rapport 2012:14, 7–12.*

Rock	Quartz monzonite	B-code 1046
Sample number	TEN062005	L-code 156
Coordinates (RT90)	6412070/1399755	
Map sheet	7D SE Ulricehamn	
Locality	Tokeryd	
Project	Bedrock and bedrock quality mapping, Jönköping, scale 1:50 000	SGU project number: 80015

Aim of study

The easternmost part of the Sveconorwegian orogen is dominated by rocks belonging to the Transscandinavian Igneous Belt (TIB, Högdahl et al. 2004). The TIB consists of large batholiths composed of granite–syenitoid–dioritoid–gabbroid rocks and associated volcanic equivalents. Ages range between 1.85 and 1.65 Ga (Högdahl et al. 2004 and references therein) and show an overall southward to south-westward younging trend. The TIB has been divided into three age groups: TIB-1 at 1.81–1.76 Ga, TIB-2 at 1.71–1.68 Ga and TIB-3 at 1.67–1.65 Ga (Larson & Berglund 1992). In the Jönköping area, TIB-1 rocks principally occur in the eastern part whereas the south-western and western areas principally expose TIB-2 rocks (e.g. Wik et al. 2006, Eliasson et al. 2008, Appelquist et al. 2009).

This study presents U-Pb data for zircon from a quartz monzonite that is exposed as several small bodies situated some 15 km north-north-west of Jönköping (Larson & Berglund 1995). The adjacent rocks to the east are dark grey, microcline porphyritic granite to quartz monzodiorite belonging to TIB-1. TIB-2 rocks, mainly microcline porphyritic granites (Barnarp type) with small intrusions of reddish, equigranular TIB-2 granites, occur farther to the west and south. The majority of these rocks are fairly well preserved igneous rocks. Deformation increases towards the south-west and a gneissosity becomes visible in the TIB-2 granites. Strong ductile deformation is mainly restricted to the contact zone between the TIB-1 and TIB-2 units and it is interpreted to predate the north–south trending steep to sub-vertical discrete deformation zones characteristic for deformation in the Protogine Zone (Wik et al. 2006).

The aim of this study is to date the igneous crystallisation of quartz monzonite bodies along the stipulated contact zone between TIB-1 and TIB-2 intrusions in the Jönköping area to constrain the western extension of TIB-1 rocks.

Sample description

The dated quartz monzonite is reddish grey, coarsely medium-grained, isotropic to weakly foliated and non-equigranular to porphyritic with less than 15 mm large microcline ± plagioclase phenocrysts (Fig. 1). In addition to the felsic minerals the rock contains biotite (c. 12 vol%), hornblende

Figure 1. The dated quartz monzonite from Tokeryd, c. 15 km north-north-west of Jönköping.

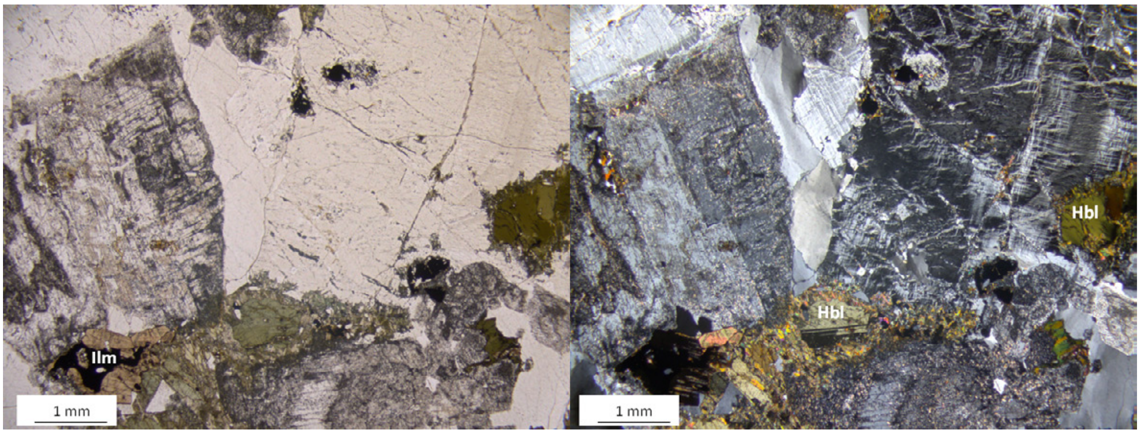

Figure 2. Photomicrographs in plane (left) and cross-polarised (right) light of the dated quartz monzonite. Plagioclase is optically clouded by fine-grained sericite and a very fine-grained saussurite assemblage of albite + epidote + calcite. The green hornblende (Hbl) is mantled by fine-grained secondary biotite. An about 1.5 mm long titanite crystal with a core of ilmenite (Ilm) is shown to the lower left.

(c. 1 vol%), titanite (c. 1 vol%), almost 1 vol% opaque minerals, principally magnetite and ilmenite, and subordinately some pyrite. Apatite, epidote and zircon are accessory phases. In thin section, zircon occurs as small (<170 µm) tabular crystals.

Plagioclase is generally severely altered to sericite and saussurite (Fig. 2). Secondary biotite occurs as mantles on hornblende and along microfractures and grain boundaries (Fig. 2).

U-Pb zircon analyses

Zircon was extracted from a c. 0.5 kg large sample of reddish-grey, almost isotropic quartz monzonite. The analytical procedures are described in the Appendix. The sample was rich in zircon and the grains are overall euhedral with sharp external terminations typical for pristine crystals not exposed to secondary alteration (Fig. 3). The zircons are short to sometimes long prismatic,

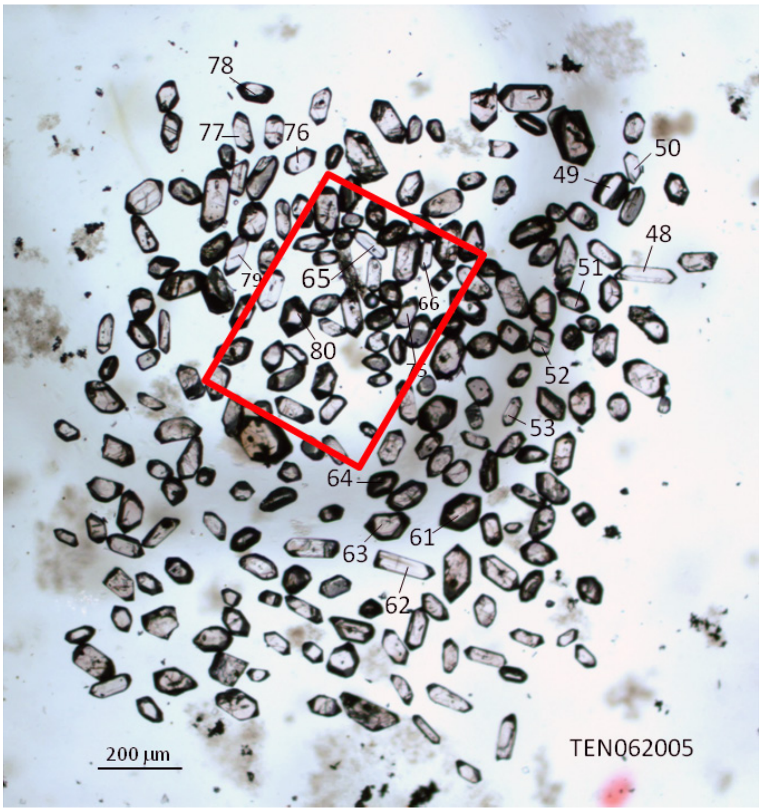

Figure 3. Optical microscope photo (plane polarised light) of representative zircon crystals from sample TEN062005 in polished section of epoxy mount used for LA-SF-ICP MS analyses. Numbers refer to analytical ID in Table 1. Note the euhedral character of the zircon population. The location of the CL-image in Fig. 4 is indicated with a red square.

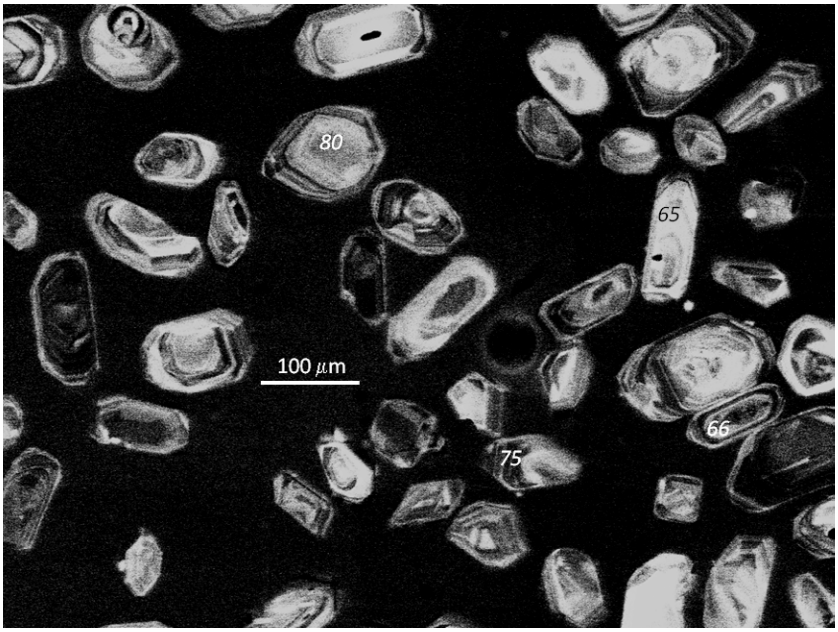

Figure 4. CL-image of the analysed zircon mount. Numbers refer to ID of spot analysed with LA-SF-ICP MS, cf. Table 1. The CL-image area is outlined in Fig. 3.

typically about 50–200 µm in size, colourless and translucent and quite commonly with a greyish cloudiness. Cracks and inclusions are sparse and turbid cores are, as a rule, absent.

In cathodoluminescence (CL) images, the zircons are oscillatory zoned (Fig. 4). The zonation continues throughout the whole crystal and secondary alteration features are subordinate.

Table 1. LA-SF-ICP MS U-Th-Pb zircon data from a quartz monzonite at Tokeryd, north-north-west of Jönköping (sample TEN062005). Analyses TEN-49 and TEN-66 were excluded from age calculation.

Sample Spot #	CL image class*	[U] ppm	Th/U calc.	$^{206}Pb/^{204}Pb$ meas.	$^{238}U/^{206}Pb$	±σ %	$^{207}Pb/^{206}Pb$	±σ %	Conc. %	$^{238}U/^{206}Pb$ age (Ma)	±σ	$^{207}Pb/^{206}Pb$ age (Ma)	±σ
TEN-48	CLB broad banded	112	1.00	8542	3.26	1.57	0.104	1.44	101	1725	23	1704	25
TEN-49	*CLB broad banded*	*43*	*0.63*	*10755*	*2.70*	*4.32*	*0.105*	*1.43*	*118*	*2029*	*76*	*1718*	*28*
TEN-50	CLB broad banded	89	0.69	7325	3.37	1.01	0.103	0.97	100	1679	16	1687	20
TEN-51	CLG broad banded	119	0.97	45224	3.34	1.00	0.104	0.96	99	1687	16	1697	18
TEN-52	CLG narrow banded	134	0.77	14363	3.13	1.10	0.104	0.96	105	1782	18	1705	18
TEN-53	CLG narrow banded	173	1.13	11131	3.61	1.62	0.105	0.95	92	1575	23	1708	16
TEN-61	CLD broad banded	239	1.42	9189	3.34	1.27	0.104	0.48	99	1688	19	1702	12
TEN-62	CLG narrow banded	130	1.39	15102	3.53	1.94	0.104	0.96	94	1607	29	1703	19
TEN-63	CLB broad banded	82	0.83	4918	3.33	1.33	0.105	0.95	98	1692	21	1719	20
TEN-64	CLG narrow banded	159	0.85	99999	3.32	0.83	0.104	0.48	99	1694	13	1705	8
TEN-65	CLB broad banded	80	0.79	11789	3.41	0.95	0.105	0.95	97	1657	13	1715	19
TEN-66	*CLG narrow banded*	*128*	*0.64*	*29066*	*3.40*	*1.53*	*0.106*	*0.94*	*96*	*1661*	*24*	*1733*	*17*
TEN-75	CLG narrow banded	99	0.70	23918	3.39	1.53	0.104	0.96	98	1668	22	1696	15
TEN-76	CLG broad banded	153	0.87	46188	3.40	0.95	0.104	0.96	98	1663	13	1695	17
TEN-77	CLG narrow banded	135	0.70	19592	3.48	1.15	0.103	0.97	97	1626	16	1678	17
TEN-78	CLB broad banded	107	0.88	10805	3.41	1.02	0.105	1.43	97	1658	16	1708	24
TEN-79	CLG narrow banded	132	0.63	14621	3.36	1.27	0.103	0.97	100	1682	17	1684	18
TEN-80	CLG broad banded	127	0.86	4648	3.50	1.22	0.103	0.97	96	1620	17	1679	14

* All analysed domains are oscillatory zoned.

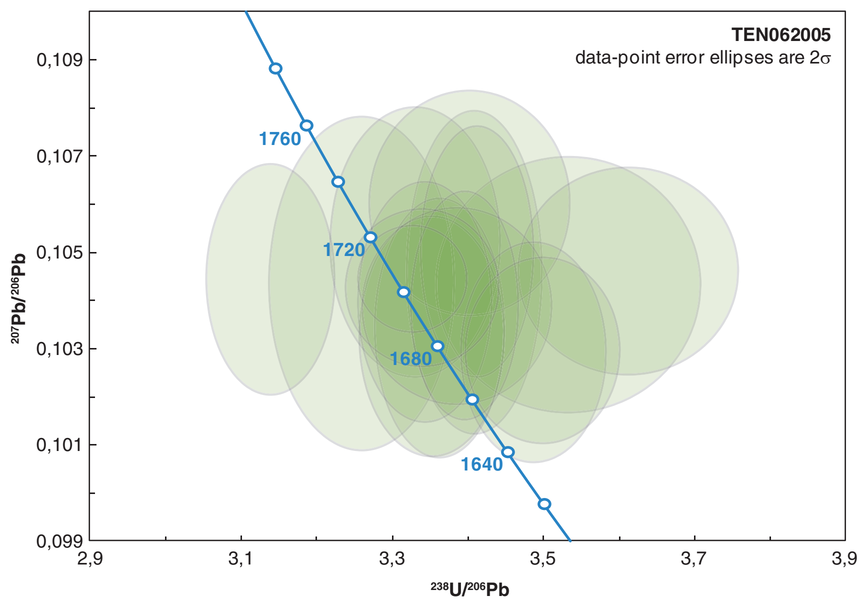

Figure 5. Tera Wasserburg Concordia plot of the sixteen U-Pb LA-SF-ICP MS analyses used for age calculation of zircon in sample TEN062005.

Results

Eighteen spot analyses were set in oscillatory zoned, euhedral, clear and translucent crystals without visible inclusions. Uranium contents and Th/U ratios of the analysed zircons are in the range 43–239 ppm and 0.63–1.42, respectively. Sixteen out of the eighteen analysed spots were used for age calculation. Two analyses were discarded from the age calculation: one analysis (TEN-49) had a too low count rate and one spot (TEN-66) burned through the crystal. Most of the remaining sixteen analyses plot concordantly at about 1700 Ma, but a slight horizontal spread of the cluster prohibits calculation of a common concordia age (Fig. 5). Together, however, the 16 spot analyses yield a well defined $^{206}Pb/^{207}Pb$ age of 1700±8 Ma (MSWD = 0.52, Fig. 6). This age is interpreted to date igneous crystallisation of zircon in the quartz monzonite.

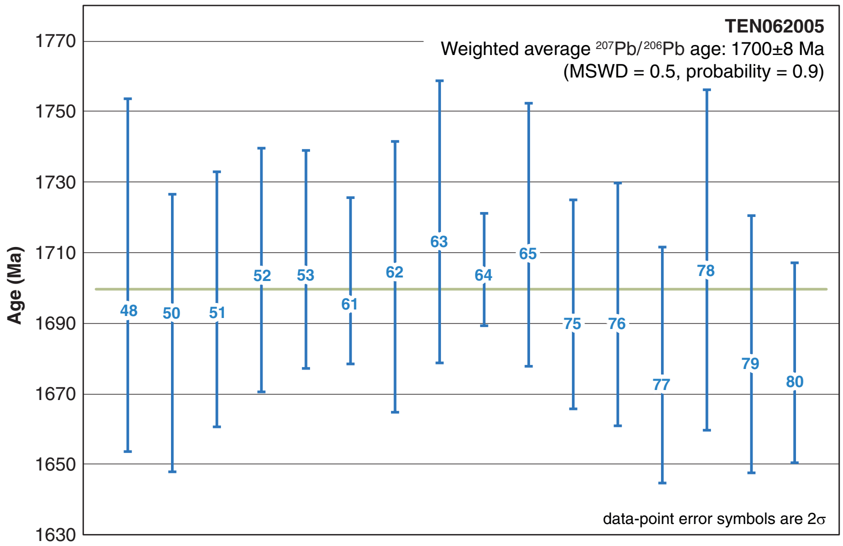

Figure 6. Plot of $^{207}Pb/^{206}Pb$ ages in million years (Ma) for the sixteen analyses used for age calculation of zircon crystallisation in sample TEN062005. Weighted average $^{207}Pb/^{206}Pb$ age (1700±8 Ma) is shown as a pale green line. Numbers on data bars refer to analytical ID in Table 1.

Discussion and conclusion

The igneous crystallisation age of 1700±8 Ma shows that the quartz monzonitic bodies in the Bankeryd area, north-west of Jönköping, intruded more or less coevally with the adjacent Barnarp-type TIB-2 granite (Gorbatschev & Bogdanova 2006) and more strongly metamorphosed 1.7 Ga old granites and syenitoids of TIB-2 and orthogneisses farther to the west (Brander et al. 2011).

References

Appelquist, K., Eliasson, T., Bergström, U. & Rimša, A., 2009: The Palaeoproterozoic Malmbäck Formation in S Sweden: age, composition and tectonic setting. *GFF 131:3*, 229–243.

Brander, L., Appelquist, K., Cornell, D & Andersson, U.B., 2011: Igneous and metamorphic geochronologic evolution of granitoids in the central Eastern Segment, southern Sweden. *International Geology Review 54:5*, 509–546, DOI:10.1080/00206814.2010.543785.

Eliasson, T., Bergström, U. & Jönberger, J., 2008: *In* Delin, H. (Ed.): Berggrundsgeologisk undersökning – sammanfattning av pågående verksamhet 2007. *Sveriges geologiska undersökning Rapport 2008:24*, 88–99.

Gorbatschev, R. & Bogdanova, S., 2006: *Aspects of the Proterozoic boundary between SE and SW Sweden. Results from SGU research project 03-1118/2000 "Proterozoic structures in Småland as a reference for coming SGU work"*. Results from SGU external research project 03-1118/2000, Unpublished Report, 51 pp. Accessed from < http://www.sgu.se/sgu/sv/fou/extern/fourapporter.html> 20120615.

Högdahl, K., Andersson, U.B. & Eklund, O., 2004: The Transscandinavian Igneous Belt in Sweden: A review of its character and evolution. *Geological Survey of Finland Special Paper 37*, 125 pp.

Larson, S.Å. & Berglund, J., 1992: A chronological subdivision of the Transscandinavian Igneous Belt – three magmatic episodes? *Geologiska Föreningens i Stockholm Förhandlingar 114*, 459–461.

Larson, S.Å. & Berglund, J., 1995: Berggrundskartan, 7D Ulricehamn SE. *Sveriges geologiska undersökning Af 178*.

Wik, N.-G., Andersson, J., Bergström, U., Claeson, D., Juhojuntti, N., Kero, L., Lundqvist, L., Möller, C., Sukotjo S. & Wikman, H., 2006: Beskrivning till regional berggrundskarta över Jönköpings län. *Sveriges geologiska undersökning K 61*, 60 pp.

U-Pb IGNEOUS PROTOLITH ZIRCON AGE OF A GRANITIC MIGMATITIC GNEISS IN THE EASTERN SEGMENT OF THE SVECONORWEGIAN OROGEN, ALINGSÅS AREA

Lena Lundqvist, Jenny Andersson & Fredrik Hellström

Lundqvist, L., Andersson, J. & Hellström, F., 2012: U-Pb igneous protolith zircon age of a granitic migmatitic gneiss in the Eastern Segment of the Sveconorwegian orogen, Alingsås area. *In* J. Andersson (Ed.): U-Pb zircon geochronology of granitic and syenitoid rocks across the southern part of the Sveconorwegian orogen. *SGU-rapport 2012:14, 13–18.*

Rock	Granitic migmatitic gneiss	SGU B-kod: 8101
Tectonic Domain	Sveconorwegian Province	
Stratigraphic position	Eastern Segment, lower unit	SGU L-kod: 907
Sample number	FRJ031048A	n1629, n1637, n1639
Coordinates	6425681/352942 (SWEREF)	6429661/1305227 (RT90)
Map sheet	64D 2fNV (SWEREF)	7C 5b (RT90)
Locality	Kvarnbacken, Alingsås	
Project	Östra Göteborg, berg, lokal	SGU project code: 1104501

Introduction

The eastern part of the Sveconorwegian orogen consists of two crustal-scale orogenic segments: (I) the parautochthonous to allochthonous Eastern Segment, adjoining the pre-Sveconorwegian foreland in the east, and (II) the allochthonous Idefjorden Terrane overlying the Eastern Segment in the west (Fig. 1). The lithotectonic boundary between the Eastern Segment and the Idefjorden Terrane is located within a west-dipping to sub-vertical, major ductile shear belt referred to as the Mylonite Zone (Stephens et al. 1996, Viola et al. 2011). These two orogenic segments show fundamentally different igneous, structural and metamorphic evolutions in both Sveconorwegian and pre-Sveconorwegian time (Bingen et al. 2008).

During the years 2003–2005, SGU conducted bedrock mapping at the scale 1:50 000 along and east of the southern shallowly west-dipping section of the Mylonite Zone, in the area of Alingsås

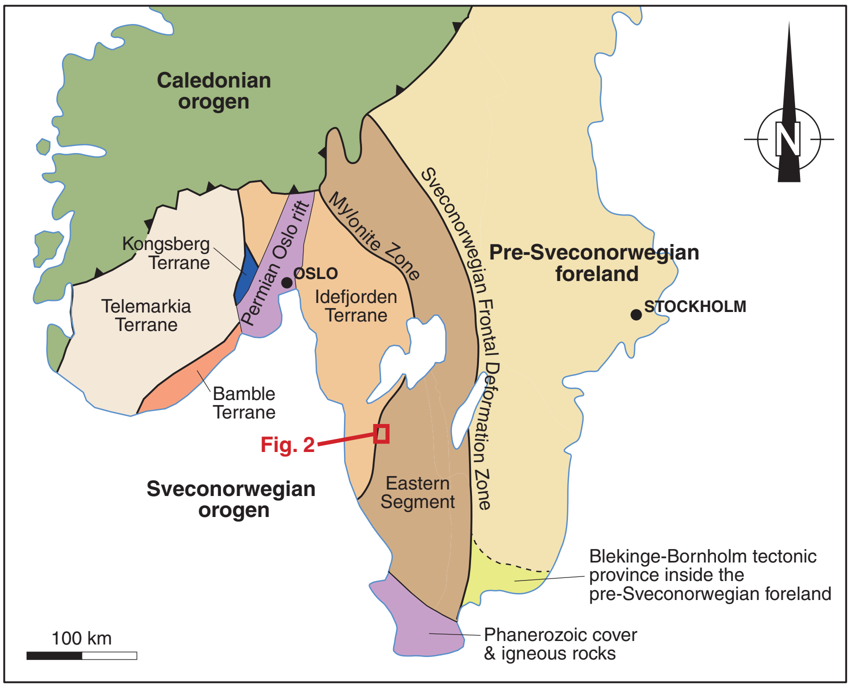

Figure 1. Schematic outline of the Sveconorwegian orogen in the southern Fennoscandian Shield. Outline of orogenic segments in Norway follows Bingen et al. (2008). Location of study area marked with red square.

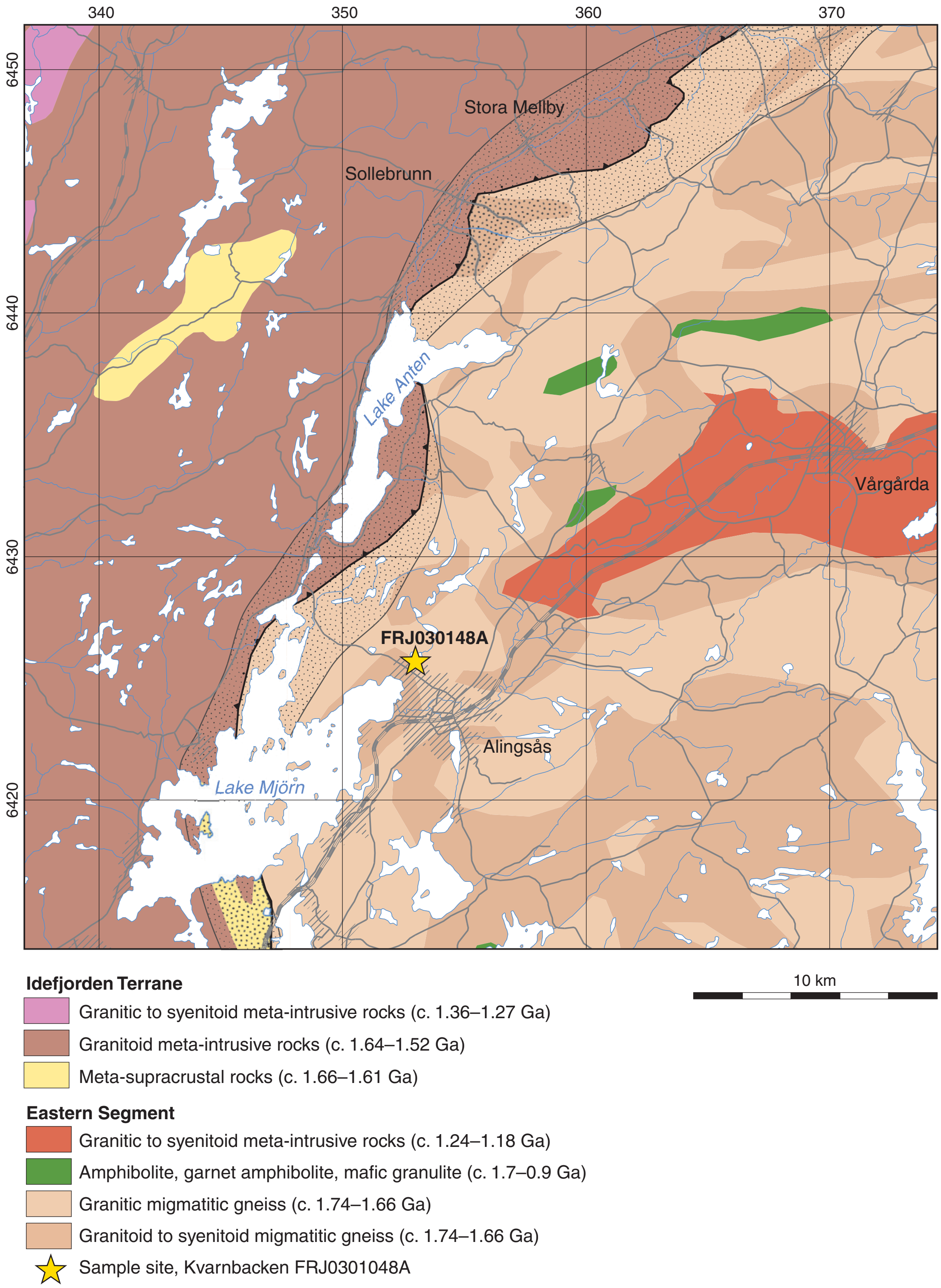

Figure 2. Geological map of the Alingsås area (data source SGU 2011, bedrock map database at the scale 1:1 million). Dotted area marks the outline of the Mylonite Zone deformation belt.

(Fig. 2, Lundqvist et al. 2005, 2006). Immediately west-south-west thereof, around Lake Mjörn, the Mylonite Zone has previously been outlined as a complex, shallowly west-dipping, up to 5 km wide deformation zone network that forms a major regional scale tectonic contact between Sveconorwegian tectonic sub-provinces (Park et al. 1991). During mapping carried out by SGU in the area of Lake Anten, lithologies on both sides of the Mylonite Zone deformation belt were identified as high-grade orthogneisses intercalated with meta-basic rocks, and the terrane affinity of the high-grade gneisses in the Alingsås area was put in question.

According to the available geochronological data, orthogneisses in the Eastern Segment have 1.74–1.65 Ga old igneous protoliths of principally granitic to syenitoid compositions (Lindh & Gorbatschev 1984, Wik et al. 2006, 2009). In contrast, orthogneiss protoliths in the Idefjorden Terrane are mainly 1.64–1.52 Ga granitoid intrusions (Åhäll & Connelly 2008). In order to test the validity of the location of the eastern boundary of the Idefjorden Terrane in the Lake Anten area (e.g. Berthelsen 1980, Park et al. 1991), a banded, migmatitic orthogneiss with a shallow dip to the north was sampled just north of the town of Alingsås for direct dating of the igneous protolith zircon. The data on the igneous protolith zircon would corroborate terrane affinity of the investigated high-grade gneiss complex.

Sample description

The sampled rock is a greyish red, compositionally banded migmatitic granitic gneiss with less than 25 vol% coarse-grained vein material. Concordant intercalations of decimeter to meter wide semi-continuous amphibolitic bands are common in this gneiss unit (Fig. 3). These bands may be remnants of mafic dyke injections or mafic enclaves. At microscale, the rock is unequigranular with irregular cusps and lobes grain-boundaries. It is a microcline-bearing leucogranitic rock with trace amounts of muscovite and less than 5 vol% mafic minerals, dominated by brown to dark beige biotite (Fig. 4A). About 50 vol% of the plagioclase is altered. Accessory phases are opaque

Figure 3. Sample locality for the dated granitic gneiss (sample FRJ031048A). Photo: Ildikó Antal Lundin, SGU.

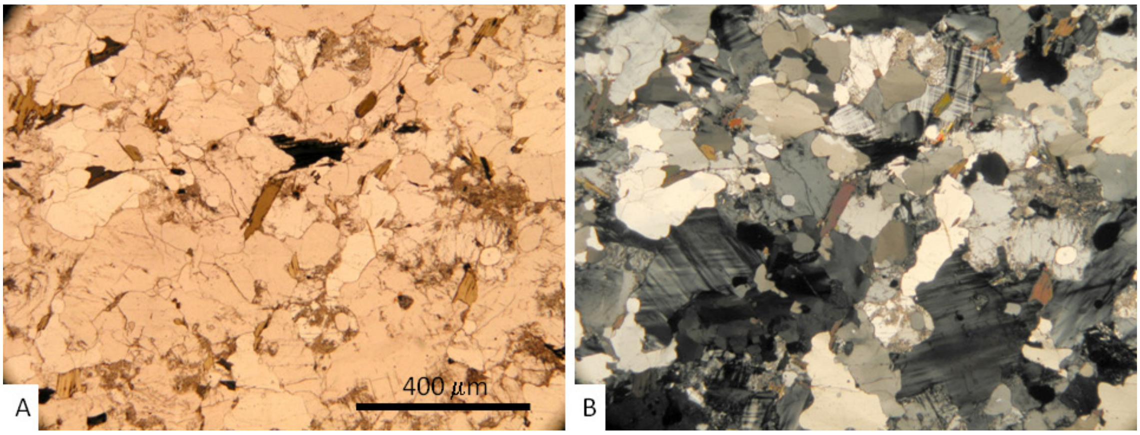

Figure 4. Photomicrograph of a thin section from the analysed sample. Crossed polars to the right.

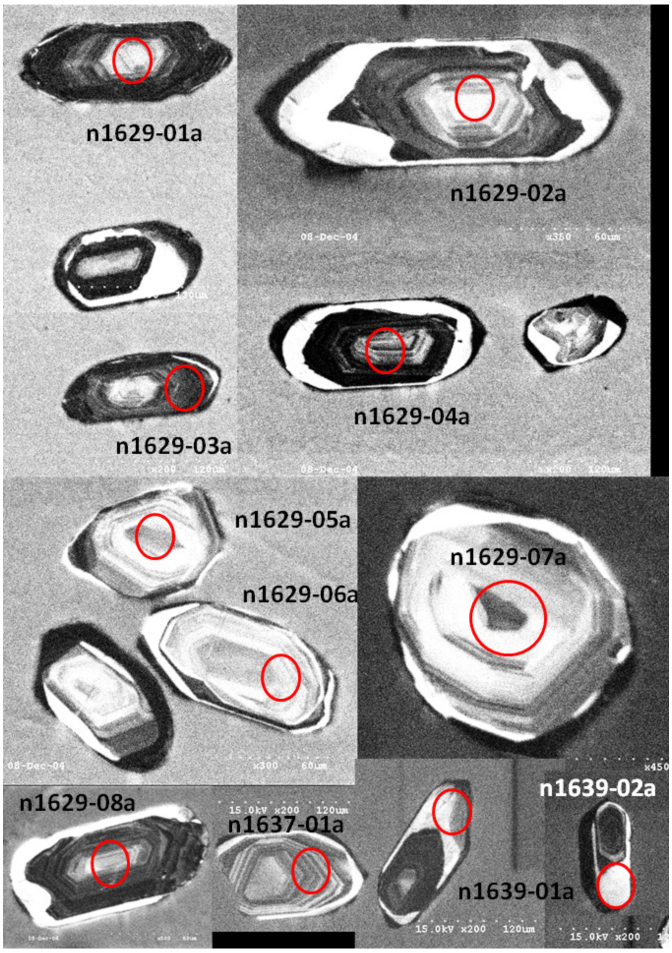

Figure 5. CL-images of zircon grains with the approximate location of spot analyses marked. Numbers refer to analytical spot number in Table 1. The spot size is c. 25 µm.

minerals, zircon and apatite. The mineralogy of the rock indicates significant retrogression at lower grade metamorphic conditions.

Analytical results and interpretation of geochronological data

Analytical procedures are described in the Appendix. U-Pb-Th SIMS analysis of zircon was performed at the NORDSIM facility at the Museum of Natural History in December 2004. The

Table 1. SIMS U-Pb-Th zircon data (FRJ031048A).

Sample/ spot #	U ppm	Pb ppm	Th/U calc.	$^{206}Pb/^{204}Pb$ measured	f_{206} %	$^{238}U/^{206}Pb$	±σ %	$^{207}Pb/^{206}Pb$	±σ %	Disc. % 2σ lim.	$^{207}Pb/^{206}Pb$ Age (Ma)	±σ	$^{206}Pb/^{238}U$ Age (Ma)	±σ
n1629-01a	152	52	0.619	13524	0.14	3.786	1.72	0.10146	0.78	−4.6	1651	14	1511	23
n1629-02a	170	66	0.822	15079	0.12	3.457	1.73	0.10241	0.80		1668	15	1638	25
n1629-03a	716	195	0.374	3068	0.61	4.487	1.68	0.09403	0.59	−11.4	1509	11	1297	20
n1629-04a	293	101	0.672	22761	0.08	3.827	1.70	0.10056	0.51	−5.5	1634	9	1497	23
n1629-05a	113	47	0.999	12911	0.14	3.323	1.73	0.09940	0.82	0.4	1613	15	1696	26
n1629-06a	115	44	0.733	10904	0.17	3.445	1.73	0.10392	0.81		1695	15	1643	25
n1629-07a	135	56	0.916	20122	0.09	3.266	1.83	0.10251	0.73		1670	13	1722	28
n1629-08a	343	120	0.589	24610	0.08	3.662	1.69	0.10085	0.46	−1.8	1640	8	1557	23
n1637-01a	111	42	0.740	21953	*0.09	3.505	1.58	0.10114	0.85		1645	16	1618	23
n1639-01a	421	83	0.089	1615	1.16	5.680	1.59	0.08927	0.82	−23.0	1410	16	1045	15
n1639-02a	216	31	0.035	743	2.52	7.719	1.58	0.07572	1.81	−17.9	1088	36	785	12

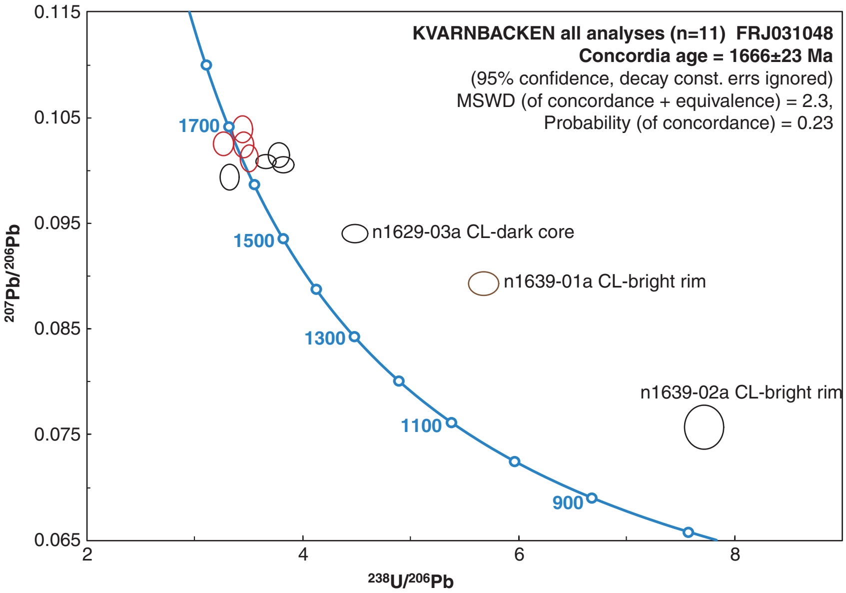

Figure 6. Tera Wasserburg diagram showing U-Pb SIMS data for zircon in the Kvarnbacken granitic gneiss. Analyses used for age calculation are shown in red.

analytical results are shown in Table 1. The zircon grains in the sample are subhedral to anhedral with oscillatory zoned cores. Cathodoluminescence (CL) images show that the zoned cores are surrounded by texturally younger unzoned and irregularly shaped CL-bright domains and thin, outer CL-dark rims (Fig. 5).

Nine analyses were aimed at oscillatory zoned core domains and two analyses at CL-bright domains. The uranium content of the zircon is 111–716 ppm. Th/U ratios are 0.37–0.94 for core analyses and 0.04–0.09 for the two rim analyses (n1639-01a, n1639-02a), which also have high values of common lead (Table 1). Four of the analyses aimed at core domains are concordant and these points give a concordia age of 1666±23 Ma (95% confidence, MSWD of concordance and equivalence = 2.3, Fig. 6). The weighted average $^{207}Pb/^{206}Pb$ age is 1670±31 Ma (95% confidence, MSWD = 1.8, probability = 0.15). The concordia age is chosen as the best age estimate suggesting igneous crystallisation of the Kvarnbacken gneiss protolith at c. 1.67 Ga.

Discussion and conclusion

Igneous crystallisation of zircon from a granitic orthogneiss at Kvarnbacken, Alingsås, was dated at 1666±23 Ma. This age is identical to igneous crystallisation of zircon in orthogneisses across the Eastern Segment of the Sveconorwegian orogen (see age compilation in Bingen & Solli 2009). This confirms earlier interpretations suggesting that the location of the lithotectonic boundary between the Eastern Segment and the Idefjorden Terrane of the Sveconorwegian orogen is to be found within the north–south trending, shallowly west-dipping high-strain deformation belt in current literature referred to as the Mylonite Zone (cf. Berthelsen 1980, Park et al. 1991, Stephens et al. 1996, Viola et al. 2011).

Acknowledgment

Martin Whitehouse, Lev Ilyinsky and Kerstin Lindén at the Nordsim analytical facility are thanked for their assistance with SIMS-analyses.

References

Åhäll, K.I. & Connelly, J.N., 2008: Long-term convergence along SW Fennoscandia: 330 m.y. of Proterozoic crustal growth. *Precambrian Research 161*, 452–474.

Berthelsen, A., 1980: Towards a palinspastic analysis of the Baltic shield. *In* J. Cogne & M. Slansky (Eds.): Geology of Europe from Precambrian to Post-Hercynian Sedimentary Basins. *Int. Geol. Congr., Colloq. C6, Paris*, 5–21.

Bingen, B. & Solli, A., 2009: Geochronology of magmatism in the Caledonian and Sveconorwegian belts of Baltica: synopsis for detrital zircon provenance studies. *Norwegian Journal of Geology 89*, 267–290.

Bingen, B., Nordgulen, Ø. & Viola, G., 2008: A four-phase model for the Sveconorwegian orogeny, SW Scandinavia. Norwegian Journal of Geology 88, 43–72.

Lindh, A. & Gorbatschev, R., 1984: Chemical variation in a Proterozoic suite of granitoids extending across a mobile belt – craton boundary. *Geologishe Rundschau 73*, 881–893.

Lundqvist, L., Andersson, J., Antal Lundin, I. & Hellström, F., 2005: Projekt Östra Göteborg, berg. *In* H. Delin (Ed.): Berggrundsgeologisk undersökning – sammanfattning av pågående verksamhet 2004. *Sveriges geologiska undersökning Rapporter och meddelanden 120*, 36–51.

Lundqvist, L., Andersson, J., Bergström, U., Hellström, F. & Antal Lundin, I., 2006: Projekt Östra Göteborg, berg. *In* H. Delin (Ed.): Berggrundsgeologisk undersökning – sammanfattning av pågående verksamhet 2004. *Sveriges geologiska undersökning Rapporter och meddelanden 123*, 52–62.

Park, R.G., Åhäll, K.-I. & Boland, M.P., 1991: The Sveconorwegian shear-zone network of SW Sweden in relation to mid-Proterozoic plate movements. *Precambrian Research 49*, 245–260.

SGU, 2011: *Bedrock – database 1:1 million*.

Stephens, M.B., Wahlgren, C.-H., Weijermars, R. & Cruden, A.R., 1996: Left-lateral transpressive deformation and its tectonic implications, Sveconorwegian orogen, Baltic Shield, southwestern Sweden. *Precambrian Research 79*, 261–279.

Viola, G., Henderson, I.H.C., Bingen, B. & Hendriks, B.W.H., 2011: The Grenvillian-Sveconorwegian orogeny in Fennoscandia: Back-thrusting and extensional shearing along the "Mylonite Zone". *Precambrian Research 189*, 368–388.

Wik, N.-G., Andersson, J., Bergström, U., Claeson, C., Juhojuntti, N., Kero, L., Lundqvist, L., Möller, C., Sukotjo, S. & Wikman, H., 2006: Beskrivning till regional bergrundskarta över Jönköpings län. *Sveriges geologiska undersökning K 61.*

Wik, N.-G., Claeson, C., Bergström, U., Hellström, F., Jelinek, C., Juhojuntti, N., Jönberger, J., Kero, L., Lundqvist, L., Sukotjo, S. & Wikman, H., 2009: Beskrivning till regional bergrundskarta över Kronobergs län. *Sveriges geologiska undersökning K 142*.

U-Pb ZIRCON AGE OF THE LATE GOTHIAN VÄTTNET GRANITE ON NORD-KOSTER IN THE IDEFJORDEN TERRANE, SOUTH-WESTERN SWEDEN

Thomas Eliasson[1], Anders Scherstén[2], Jenny Andersson[3] & Andreas Petersson[2]

[1]Geological Survey of Sweden, Guldhedsgatan 5A, SE-413 20 Göteborg, Sweden
[2]Department of geology, Lund university, Sölvegatan 12, SE-223 62 Lund, Sweden
[3]Geological Survey of Sweden, Box 670, SE-751 28 Uppsala, Sweden

Eliasson, T., Scherstén, A., Andersson, J. & Petersson, A., 2012: U-Pb zircon age of the late Gothian Vättnet granite on Nord-Koster in the Idefjorden Terrane, south-western Sweden. *In* J. Andersson (Ed.): U-Pb zircon geochronology of granitic and syenitoid rocks across the southern part of the Sveconorwegian orogen. *SGU-rapport 2012:14, 19–25*.

Rock	Granite	B-code 1058
Sample number	TEN085058B	L-code 920
Coordinates (RT90)	6541078/1224150	
Map sheet	9A NO Strömstad	
Locality	“Ground zero”, Vättnet	Nord-Koster
Project	Koster berg och jord	SGU project number: 80019

Aim of study

The Vättnet granite is exposed in the north-eastern part of the Koster archipelago. It belongs to a granitic suite that is intrusive into the migmatitic supracrustal rocks of the Stora Le-Marstrand group (SLM, Eliasson 2011). The suite comprises two textural and compositional varieties: grey, porphyritic biotite ± hornblende granite and, subordinately, a fine- to medium-grained leucogranite. The latter varies in colour from grey to red and occurs as sheets and elongated somewhat irregular intrusions within the grey porphyritic Vättnet granite.

The Vättnet granite contains xenoliths of the migmatitic SLM meta-greywacke (Fig. 1) as well as of the adjacent Gothian meta-granodiorite to meta-tonalite intrusion. Based on detailed structural studies, Hageskov (1985) concluded that the “sheeted granite” (denoted the Vättnet granite by Eliasson 2011 and in this study) is the youngest granitic intrusion in the Koster archipelago as it show no signs of deformation prior to the Sveconorwegian shearing that affected the north-eastern part of the archipelago.

Figure 1. Porphyritic Vättnet granite with a xenolith of migmatitic SLM meta-greywacke. The photograph is from Märebukterna some 1.6 km north-west of Vättnet.

The aim of the present study is to date the igneous crystallisation of the Vättnet granite and thus the cessation of magmatism in the Koster archipelago. Metamorphosed and deformed dolerite dykes are abundant in the granite (Koster dykes, Hageskov 1985). Thus, the age of the granite will provide important information on the maximum age of the Koster dykes.

Regional geology

The Koster islands are located in the westernmost part of the Østfold-Marstrand belt in the Idefjorden Terrane of the Sveconorwegian orogen (Berthelsen 1980, Bingen et al. 2008). The oldest lithological unit in the Koster archipelago is a meta-greywacke with minor intercalations of mafic meta-volcanic rocks of the SLM group.

During the Gothian orogeny, approximately 1545 and 1520 Ma ago (Åhäll & Connelly 2008), the pervasively migmatitic SLM meta-greywacke was intruded by a number of plutonic rocks ranging in composition from gabbro to granite. The plutonic rocks were subsequently deformed and metamorphosed during the final stage of the Gothian orogeny. The dense tholeiitic Koster dyke swarm intruded in post-Gothian time as indicated by the obtained Rb-Sr age of 1421±25 Ma (Hageskov & Pedersen 1988). These dykes have been correlated with the Kattsund dyke swarm in the Sandbukta-Mølen area within Oslofjorden (Hageskov 1985) and with the 1457±6 Ma Orust dykes some 85 km to the south (Daly et al. 1983, Åhäll & Connelly 1998).

The bedrock in the north-eastern part of the Koster archipelago was intensely deformed and metamorphosed during the Sveconorwegian orogeny at 1150 to 900 Ma. The south-western part of the Koster archipelago, however, escaped much of this reworking and thus exposes a unique window into the pre-Sveconorwegian history of south-western Fennoscandia where the Gothian orogenic evolution can be studied.

Sample description

The dated sample of Vättnet granite is a grey, porphyritic, lineated and weakly gneissic biotite ± hornblende granite. The sample was selected in blasted outcrops from a construction site at Vättnet at the north-eastern part of Nord-Koster Island. The pronounced lineation is mainly defined by elongated clusters of biotite ± hornblende and by the preferred orientation of elongated microcline and plagioclase porphyroclasts (Figs. 2 & 3).

In more strained zones, porphyroclasts or augen consist of 4 to 10 mm large plagioclase and microcline crystals in a fine-grained to finely medium-grained matrix principally composed of more or less recrystallised quartz, plagioclase and K-feldspar with some biotite and hornblende (Fig. 4). Highly strained plagioclase porphyroclasts are recrystallised to multicrystalline grains.

The granite has a relatively high content of mafic minerals. Biotite predominates (c. 13.5 vol%) over amphibole (1.1 vol%) and some 20 percent of the biotite is altered to chlorite. Microcline is commonly fresh and unaltered, whereas plagioclase is severely clouded by sericite and a very fine-grained albite + epidote + calcite saussurite assemblage (Fig. 4). Accessory pyrite is the only opaque mineral found in the dated granite.

Zircon occurs as 0.01 to 0.25 mm long euhedral grains essentially found in the aggregates of biotite ± hornblende. Garnet (c. 0.7 vol%) commonly occurs in clusters of mafic minerals.

U-Pb zircon analyses

Zircon was extracted from a c. 0.5 kg large sample of the Vättnet granite. The analytical procedures are described in the Appendix. The sample was rich in zircon and the crystals were of high

Figure 2. The dated Vättnet granite from Nord-Koster (TEN085058B). The L-fabric is seen parallel (A) and perpendicular (B) to the stretching direction. Length of sample c. 10.5 cm.

Figure 3. A rock surface oriented roughly parallel to the stretching lineation of the porphyritic Vättnet granite some 30 m west of the sampling locality.

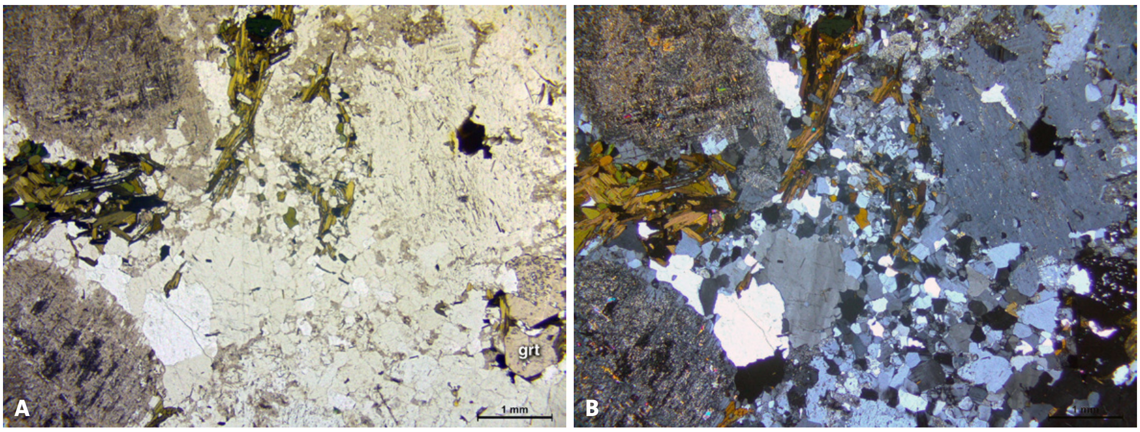

Figure 4. Photomicrograph in plane-polarised (A) and crossed-polarised (B) light of the dated porphyritic and lineated Vättnet granite. In the lower right part of the photographs are two grains of garnet (grt). The thin section is cut perpendicular to the L-fabric.

analytical quality (Fig. 5). The zircons are short to long prismatic and mostly euhedral with sharp crystal terminations that appear unaffected by secondary abrasion. They are typically colourless, translucent and clear. Cracks and inclusions are sometimes present but indications of complex core-rim relations are lacking.

In cathodoluminescence (CL) images, the crystals show oscillatory zonation that vary from narrow and thinly laminated to wide broad banded domains (Fig. 6). The oscillatory zonation typically continues all the way to the crystal margin and complex core-rim zonations are not recorded. Some grains show signs of convoluted zonation.

Results

Twenty analyses were obtained from twenty different crystals. The location of analytical spots is shown in Figure 5. Analytical data is given in Table 1. The analysed zircon is somewhat low in uranium, between 39 and 197 ppm, and have Th/U ratios between 0.33 and 0.67. The twenty

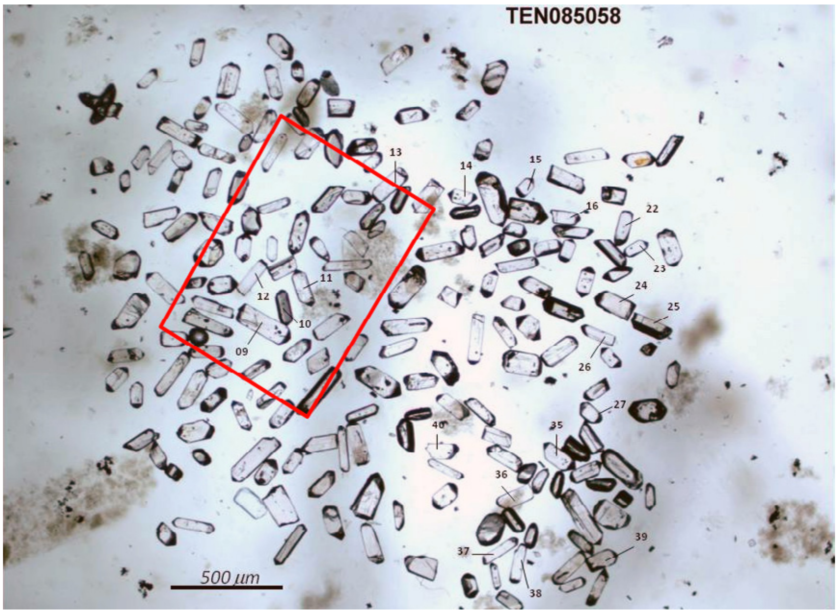

Figure 5. Optical microscope photo (plane-polarised light) of representative zircon crystals from the Vättnet granite (sample TEN085058B) in polished section of epoxy mount used for LA-SF-ICP MS analyses. Numbers refer to analytical ID in Table 1. Note the sharp euhedral character of the crystals and the translucent and clear nature of the grains in the analysed population. The location of the CL-image in Figure 6 is indicated with a red square.

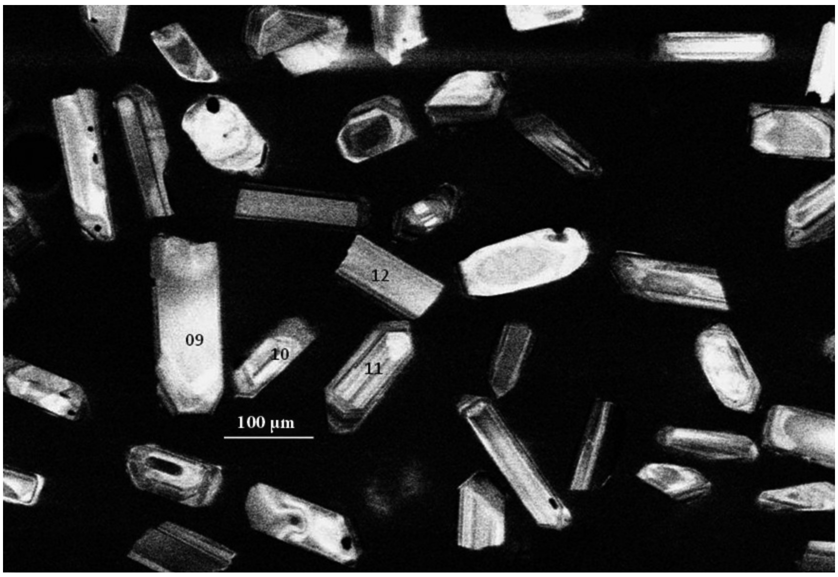

Figure 6. CL-image of analysed zircon mount from the Vättnet granite (TEN085058B). Numbers refer to ID of spot analysed with LA-SF-ICP MS, cf. Table 1. The CL-image area is outlined in Figure 5.

Table 1. LA-SF-ICPMS U-Th-Pb zircon data from the Vättnet meta-granite at Nordkoster Island (sample TEN085058B).

Sample Spot #	CL image class*	[U] ppm	Th/U calc.	$^{206}Pb/^{204}Pb$ meas.	$^{238}U/^{206}Pb$	±σ %	$^{207}Pb/^{206}Pb$	±σ %	Conc. %	$^{238}U/^{206}Pb$ age (Ma)	±σ	$^{207}Pb/^{206}Pb$ age (Ma)	±σ
TEN B-09	CLB broad banded osc	55	0.49	2118	3.75	2.16	0.094	1.60	101	1526	27	1508	26
TEN B-10	CLB broad banded osc	90	0.63	4413	3.88	1.26	0.095	1.58	96	1480	16	1538	27
TEN B-11	CLB broad banded osc	101	0.57	12239	3.57	1.35	0.094	1.06	106	1592	19	1504	21
TEN B-12	CLB broad banded osc	128	0.58	15374	3.70	2.69	0.095	1.05	101	1543	36	1522	18
TEN B-13	CLB broad banded osc	83	0.59	2357	3.91	1.27	0.094	1.06	97	1471	15	1511	19
TEN B-14	CLB broad banded osc	75	0.62	4078	3.80	2.76	0.095	1.58	98	1504	36	1532	25
TEN B-15	CLB broad banded osc	136	0.54	2512	3.73	2.61	0.095	1.05	100	1529	37	1528	15
TEN B-16	CLD narrow osc	103	0.65	2816	4.05	1.01	0.095	1.05	93	1425	13	1525	19
TEN B-22	CLD narrow osc	140	0.33	2799	3.91	0.88	0.095	0.53	96	1471	12	1531	15
TEN B-23	CLB broad banded osc	39	0.67	1766	3.62	2.27	0.094	1.06	104	1573	31	1509	20
TEN B-24	CLG narrow osc	77	0.57	3961	3.89	2.0	0.096	1.04	96	1472	27	1539	23
TEN B-25	CLG narrow osc	170	0.66	51537	3.94	1.28	0.096	1.04	94	1459	17	1556	23
TEN B-26	CLD narrow osc	185	0.46	8952	3.75	0.94	0.094	1.06	101	1524	13	1514	24
TEN B-27	CLG narrow osc	118	0.59	3154	3.94	1.28	0.093	1.61	98	1460	16	1495	26
TEN B-35	CLG narrow osc	197	0.39	99999	3.85	1.0	0.094	1.06	99	1490	12	1509	22
TEN B-36	CLB narrow osc	169	0.51	5199	3.76	0.85	0.094	1.06	101	1521	11	1511	23
TEN B-37	CLB broad banded osc	96	0.59	6491	3.83	1.34	0.094	1.60	98	1494	18	1517	29
TEN B-38	CLB broad banded osc	88	0.58	2553	3.95	2.0	0.094	1.06	97	1456	26	1499	21
TEN B-39	CLG narrow osc	134	0.35	15041	3.86	1.26	0.094	1.06	98	1485	16	1516	16
TEN B-40	CLB broad banded osc	80	0.54	2979	4.13	1.96	0.094	1.06	93	1397	23	1504	20

* All analysed domains are oscillatory zoned.

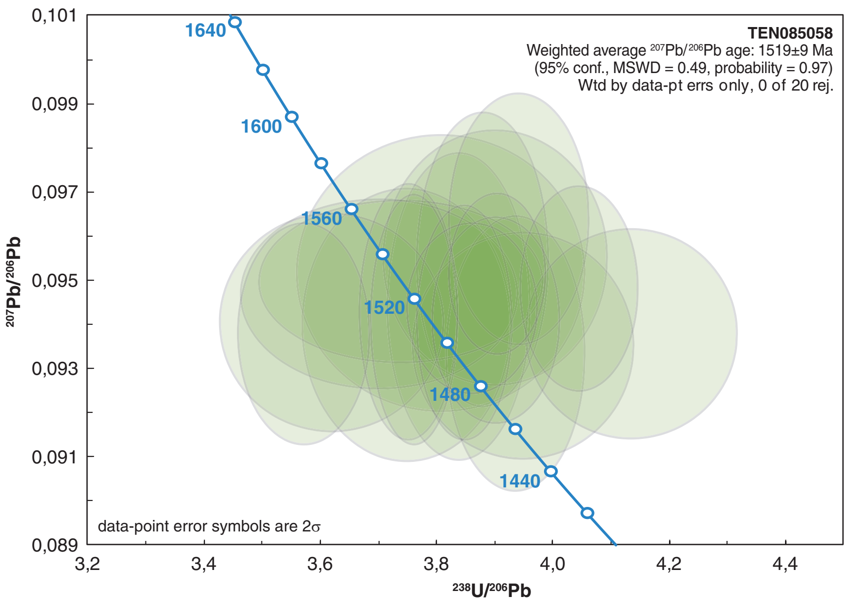

Figure 7. Tera Wasserburg Concordia plot of the twenty U-Pb LA-SF-ICP MS analyses obtained from zircon from the Vättnet meta-granite (TEN085058B).

analyses cluster on or close to the concordia, but are not equivalent enough to define a common concordia age. Together the twenty analyses define a $^{206}Pb/^{207}Pb$ age of 1519±9 Ma (MSWD = 0.51, 95% conf., Figs. 7 & 8).

The euhedral character of the crystals and the overall undisturbed, pervasive internal oscillatory zonation pattern of the analysed zircon sample suggest that post-igneous disturbance of the zircon system was negligible. The obtained $^{206}Pb/^{207}Pb$ age of 1519±9 Ma for the oscillatory zoned euhedral zircon population is interpreted to date the igneous crystallisation of the Vättnet granite. The zircon population in the granite records no inheritance of the side rock or protolith rock. This suggests that the granite magma was highly aggressive to protolith zircon or that the zircon bearing wall rocks are not a contributing source to the granite magma.

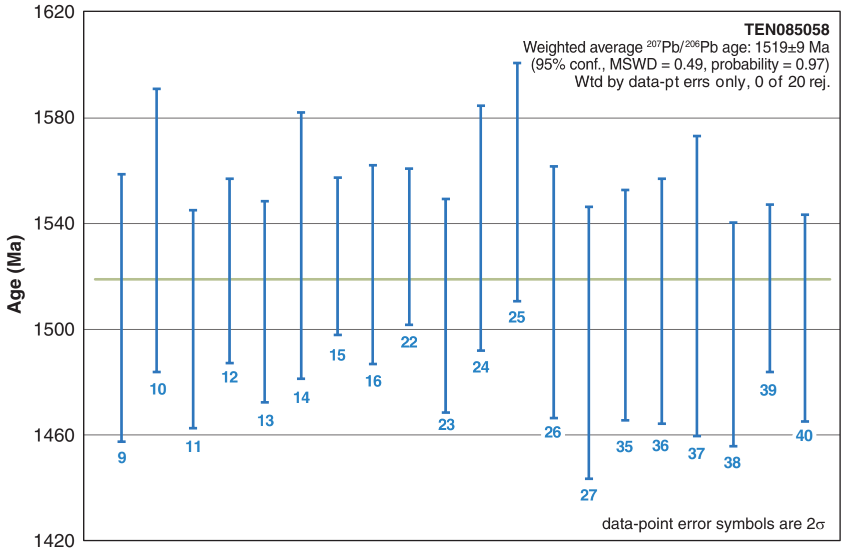

Figure 8. Plot of $^{207}Pb/^{206}Pb$ ages in million years (Ma) for the twenty analyses obtained from zircon in the sampled Vättnet granite (TEN085058B). Weighted average $^{207}Pb/^{206}Pb$ age is shown as a green line. Numbers refer to ID of spot analysed with LA-SF-ICP MS, cf. Table 1.

Discussion and conclusion

Hageskov & Mørch (2000) classified the Vättnet granite as an anorogenic intrusion. The 1519±9 Ma age for igneous crystallisation of the Vättnet granite shows that it intruded during the final stage of the Gothian orogeny. Thus, the Vättnet granite is basically synchronous with the youngest Gothian intrusions in the Idefjorden Terrane of the Sveconorwegian orogen, i.e. the 1522±10 Ma Stenungsund granodiorite in the Hisingen suite (Åhäll & Connelly 2008).

The present study proves that the granite intruded at least 60 Ma before the intrusion of the Koster dykes. The latter formed when the Gothian crust was stabilised and responded in a brittle manner to crustal extension.

References

Åhäll, K.I. & Connelly, J.N., 1998: Intermittent 1.53–1.13 Ga magmatism in western Baltica; age constraints and correlations within a postulated supercontinent. *Precambrian Research 92*, 1–20.

Åhäll, K.I. & Connelly, J.N., 2008: Long-term convergence along SW Fennoscandia: 330 m.y. of Proterozoic crustal growth. *Precambrian Research 161*, 452–474.

Berthelsen, A., 1980: Towards a palinspastic analysis of the Baltic shield. *In* J. Cogne & M. Slansky (Eds.): Geology of Europe from Precambrian to Post-Hercynian Sedimentary Basins. *Int. Geol. Congr., Colloq. C6, Paris*, 5–21.

Bingen, B., Nordgulen, Ø. & Viola, G., 2008: A four-phase model for the Sveconorwegian orogeny, SW Scandinavia. *Norwegian Journal of Geology 88*, 43–72.

Daly, J.S., Park, R.G. & Cliff, R.A., 1983: Rb-Sr isotopic equilibrium during Sveconorwegian (=Grenville) deformation and metamorphism of the Orust dykes, S.W. Sweden. *Lithos 16*, 307–318.

Eliasson, T., 2011: *Berggrundskarta, Kosterhavet Geoturistkarta, Dokumentation av de svenska nationalparkerna.* Naturvårdsverket och Sveriges geologiska undersökning 26, ISBN 978-91-620-8499-8.

Hageskov, B., 1985: Constrictional deformation of the Koster dyke swarm in a ductile sinistral shear zone, Koster islands, SW Sweden. *Bulletin of the Geological Society of Denmark 34*, 151–197.

Hageskov, B. & Mørch, B., 2000: Adakitic high-Al trondhjemites in the Proterozoic Østfold-Marstrand Belt, W Sweden. *Bulletin of the Geological Society of Denmark 46*, 165–174.
Hageskov, B. & Pedersen, S., 1988: Rb–Sr age of the Kattsund–Koster dyke swarm in the Østfold–Marstrand belt of the Sveconorwegian Province, W Sweden–SE Norway. *Bulletin of the Geological Society of Denmark 37*, 51–61.

APPENDIX: U-Pb ZIRCON ANALYSES

Zircon mineral separates were obtained by density separation of about 0.5 kg of rock sample ground to a fine powder using a swing mill and then loaded on a Wilfley water table. The magnetic minerals were removed from the heavy residue by hand magnet. Zircons were hand-picked under a stereomicroscope and about 100–200 crystals from each sample were mounted on double-faced tape. The 1065 Ma Geostandards zircon 91500 (Wiedenbeck et al. 1995) was added to the mount used for ion microprobe SIMS analysis. The mounts were cast in transparent epoxy resin and well after hardening polished to expose the central parts of the crystals. Cathodoluminescence imaging was performed on polished, gold-coated mounts using a Gatan CL3 detector on a Hitachi S-4300 electron microscope at the Swedish Museum of Natural History and a Philips X30 FEH scanning electron microscope at Stockholm University.

LA-SF-ICP-MS analyses

Zircon ages were obtained using a laser-ablation sector field inductively coupled plasma mass spectrometer (LA-SF-ICP-MS) at the Department of Geological Mapping, Geological Survey of Denmark and Greenland (GEUS). The laser ablation microprobe uses a focused laser beam to ablate a small amount of a sample contained in an air-tight sample cell. Detailed analytical protocols are described by Gerdes & Zeh (2009) and Frei & Gerdes (2009), but a brief summary is given here.

Samples and standards were mounted in a low-volume ablation cell specially developed for U-Pb-dating (Horstwood et al. 2003). Helium was used to flush the sample cell and was mixed downstream with the argon sample gas of the mass-spectrometer. A NewWave Research®/Merchantek® UP213 laser ablation unit was used that emits a beam wavelength of 213 nm and a 10 Hz repetition rate. For the spot diameter (20 µm) and ablation times (30 s) used here, the ablated mass of zircon was typically between 150 and 300 ng. The ablated material was transferred to the mass-spectrometer in an Ar-He carrier gas via Tygon® tubing into an Element2 (ThermoFinnigan®, Bremen) single-collector double focusing magnetic sector ICP-MS. The total acquisition time for each analysis was 60 s of which the first 30 s were used to determine the gas blank.

The instrument was tuned to give large, stable signals for the ^{206}Pb and ^{238}U peaks, low background count rates (typically around 150 counts per second for ^{207}Pb) and low oxide production rates ($^{238}U^{16}O/^{238}U$ generally below 2.5%). ^{202}Hg, $^{204}(Pb + Hg)$, ^{206}Pb, ^{207}Pb, ^{208}Pb, ^{232}Th and ^{238}U intensities were determined through peak jumping using electrostatic scanning in low resolution mode and with the magnet resting at ^{202}Hg. Each peak was determined at four slightly different masses and integrated sampling and a settling time of 1 ms for each isotope. Mass ^{202}Hg was measured to monitor the ^{204}Hg interference on ^{204}Pb where the $^{202}Hg/^{204}Hg \equiv 4.36$, which can be used to correct significant common lead contributions using the model by Stacey & Kramers (1975). $^{207}Pb/^{235}U$ was calculated from the $^{207}Pb/^{206}Pb$ and $^{206}Pb/^{238}U$ assuming $^{238}U/^{235}U \equiv 137.88$.

The laser induced elemental fractionation and the instrumental mass bias on measured isotopic ratios were corrected through standard-sample bracketing using the GJ-1 zircon (Jackson et al. 2004). Samples were analysed in sequences where three standards bracket each set of ten samples. The Plesovice zircon standard (Aftalion et al. 1989) has been used as an external reproducibility check, and yield long-term 2σ RSD precisions (n=109) of 2%, 2.3% and 1.1% for the $^{206}Pb/^{238}U$, $^{207}Pb/^{235}U$ and $^{207}Pb/^{206}Pb$ ratios respectively (Frei et al. 2006). The raw data is corrected for instrumental mass bias and laser-induced U-Pb fractionation through normalisation to the GJ-1 zircon using in-house data reduction software.

All isotope data were plotted and evaluated using ISOPLOT/EX 3.06 (Ludwig 2003). Model age calculation and error propagation follows Sambridge & Lambert (1997).

U-Pb ion microprobe (SIMS) analyses

High-spatial resolution secondary ion masspectrometer (SIMS) analysis was made using a Cameca IMS 1270 at the Nordsim facility at the Swedish Museum of Natural History in Stockholm. Detailed descriptions of the analytical procedures for these analyses are given in Whitehouse et al. (1999) and Whitehouse & Kamber (2005). The instrument was operating with a spot size less than 25 µm. Age calculations of isotopic data were made using software Isoplot 3.00 (Ludwig 2003). The amount of common ^{206}Pb in measured ^{206}Pb is estimated from ^{204}Pb assuming a present day terrestrial lead following the model of Stacey & Kramers (1975). Statistical precisions of age estimates are given at the 2σ level (unless otherwise explicitly stated).

References

Aftalion, M., Bowes, D.R. & Vŕana, S., 1989: Early Carboniferous U-Pb zircon ages for garnetiferous perpotassic granulites, Blanský les massif, Czechoslovakia. *Neues Jahrbuch Mineralogie, Monatshefte 4*, 145–152.

Frei, D. & Gerdes, A., 2009: Precise and accurate in situ U-Pb dating of zircon with high sample throughput by automated LA-SF-ICP-MS. *Chemical Geoology 261*, 261–270.

Frei, D., Hollis, J.A., Gerdes, A., Harlov, D., Karlsson, C., Vasquez, P., Franz, G., Johansson, L. & Knudsen, C., 2006: Advanced in-situ trace element and geochronological microanalysis of geomaterials by laser ablation techniques. *Geological Survey of Denmark and Greenland Bulletin 10*, 25–28.

Gerdes, A. & Zeh, A., 2009: Zircon formation versus zircon alteration — new insights from combined U-Pb and Lu-Hf in-situ LA-ICP-MS analyses, and consequences for the interpretation of Archean zircon from the Central Zone of the Limpopo Belt. *Chemical Geology 261*, 230–243. doi:10.1016/j.chemgeo.2008.03.005.

Horstwood, A.S.A., Foster, G.L., Parrish, R.R., Noble, S.R. & Nowell, G.M., 2003: Common-Pb corrected in situ U-Pb accessory mineral geochronology by LA-MC-ICP-MS. *Journal of Analythical and Atomic Spectrometry 18*, 837–846.

Jackson, S.E., Pearson, N.J., Griffin, W.L. & Belousova, E.A., 2004: The application of laser ablation-inductively coupled plasma-mass spectrometry to in situ U-Pb zircon geochronology. *Chemical Geology 211*, 47–69.

Ludwig, K.R., 2003: Isoplot/Ex 3.00. *A Geochronological Toolkit for Microsoft Excel*. Special Publication, vol. 4. Berkeley Geochronological Center, Berkely, CA.

Sambridge, M. & Lambert, D.D., 1997: Propagating errors in decay equations: Examples from the Re-Os isotopic system. *Geochimica et Cosmochimica Acta 61*, 3019–3024.

Stacey, J.S. & Kramers, J.D., 1975: Approximation of terrestrial lead isotope evolution by a two-stage model. *Earth and Planetary Science Letters 26*, 207–221.

Whitehouse, M.J. & Kamber, B.S., 2005: Assigning dates to thin gneissic veins in high–grade metamorphic terranes: a cautionary tale from Akilia, Southwest Greenland. *Journal of Petrology 46*, 291–318.

Whitehouse, M.J., Kamber, B., & Moorbath, S., 1999: Age significance of U-Th-Pb zircon data from early Archaean rocks of west Greenland – a reassessment based on combined ion-microprobe and imaging studies. *Chemical Geology 160*, 201–224.

Wiedenbeck, M., Allé, P., Corfu, F., Griffin, W.L., Meier, M., Oberli, F., von Quadt, A., Roddick, J.C., & Spiegel, W., 1995: Three natural zircon standards for U-Th-Pb, Lu-Hf, trace element and REE analysis. *Geostandards Newsletter 19,* 1–23.